



Enhanced Dielectric Performance of Polyaniline-Binary Transition Metal Composites

C. ANJU^{1,3} and SHINY PALATTY^{2,4}

1.—Department of Basic Sciences and Humanities, Rajagiri School of Engineering & Technology, Ernakulam, Kerala 682039, India. 2.—Department of Chemistry, Bharata Mata College, Ernakulam, Kerala 682021, India. 3.—e-mail: anju.chonat@gmail.com. 4.—e-mail: shinypalaty@gmail.com

Polyaniline-metal composite incorporating binary transition metals was synthesized by in situ rapid mixing polymerization. The current article investigates the dielectric performance of polyaniline composite synthesized using ferric nitrate oxidant by a dopant-free template-free method and also the role of Cu^{2+} as an external redox additive in enhancing the dielectric performance of a PANI composite. The experimental results proved that the coordination of PANI nitrogen with binary transition metals (Fe & Cu) not only improved the electrical conductivity, but also augmented the dielectric performance. Also, morphological analysis substantiates the role of external Cu^{2+} additive in modifying the PANI surface to act as an efficient dielectric material.

Key words: Conducting polymers, dielectrics, energy storage and conversion, electrical properties

INTRODUCTION

With the improvement of capacitor innovation, there has been incredible headway in dielectric materials with high energy density. Because of good mechanical flexibility, high breakdown voltage and ease of synthesis, high dielectric constant polymer composites have gained much attraction^{1,2} in energy storage devices. Among such composites, the high dielectric permittivity of metal-organic systems arises from the long-range polaron hopping² mechanism. Conductive polymers have pulled in much enthusiasm for use in vitality applications in light of many beneficial qualities such as tunable electrical properties, flexibility, and high processability from solution. The fascinating virtues such as facile synthesis, reversible reaction behaviour, good electrical conduction and high dielectric permittivity ($\epsilon' \approx 10^2 - 10^3$) makes polyaniline a promising candidate as a dielectric material.^{3,4} The presence of two interconvertible benzenoid and quinoid rings by electron transfer, porous nature

and high surface area makes PANI a good pseudo-capacitive material.⁵ The poor cyclic stability due to mechanical degradation by the large volumetric change in the doping/dedoping process limits the use of PANI in many energy storage applications.⁶ Doping with transition metal ions such as Cu^{2+} , Zn^{2+} , Fe^{2+} and Co^{2+} could substantially enhance capacitance and energy density of conducting polymers.⁷ Because of the synergistic combination of the high-breakdown electric field of the polymer matrices and high dielectric permittivity of the fillers, such combinations receive extraordinary consideration.⁵ The practical performance of PANI can be effectively improved by such combinations. Because of unique electron exchange property, transition metal ion-doped PANI has gained an intensive interest in recent years since the electrical properties of PANI can be transmuted in a wide range of areas, from insulators to metallic conductors, due to the increase in charge delocalization in the polymer backbone on doping.⁵

The nature of oxidants also has a great impact in tuning the performance of PANI. For the synthesis of PANI, ammonium persulfate (APS), potassium dichromate ($\text{K}_2\text{Cr}_2\text{O}_7$), ferric chloride (FeCl_3), potassium permanganate (KMnO_4) and composite

(Received December 6, 2018; accepted July 23, 2019)

oxidants such as Fe^{3+} /hydrogen peroxide (H_2O_2) and $\text{Cu}^{2+}/\text{O}_2$ have been reported as efficient oxidants.⁸ Researchers are also interested in oxidants that can act both as oxidant and dopant. The iron-based oxidants such as $\text{Fe}_2(\text{SO}_4)_3$ have been reported by Wan and co-workers, which, on hydrolysis, produces sulphuric acid and serves as a dopant.⁹ Not much work has been reported in the synthesis of PANI using ferric nitrate oxidant. Doped polyaniline can be easily obtained without any externally added dopants with ferric nitrate because ferric nitrate anions formed during the reaction can be easily connected to imine nitrogen.⁹ The present work investigates the role of external transition metal additive in enhancing the storage performance of PANI using ferric nitrate oxidant.

EXPERIMENTAL SECTION

Materials

Aniline was double-distilled prior to use. $\text{Fe}(\text{NO}_3)_3 \cdot 9\text{H}_2\text{O}$, $\text{CuSO}_4 \cdot 5\text{H}_2\text{O}$ and acetone were of analytical grade and were used without any treatment.

Synthesis of Polyaniline Composite Using Ferric Nitrate Oxidant Without an External Redox Additive

Polyaniline was prepared by using $\text{Fe}(\text{NO}_3)_3$ oxidant (also can act as dopant) by rapid mixing chemical oxidative polymerization without an external redox additive. A 0.1 M aniline solution was prepared and was stirred using a magnetic stirrer for 15 min. To that, 0.3 M $\text{Fe}(\text{NO}_3)_3$ solution was rapidly added, and the reaction was kept overnight without any agitation. A dark green precipitate of polyaniline was filtered by using a vacuum pump and then washed with distilled water and acetone until the filtrate become colourless. Finally, it was dried in an air oven at 80°C for 24 h.

Synthesis of Polyaniline Composite Using Ferric Nitrate Oxidant with an External Redox Additive

Polyaniline was prepared by using $\text{Fe}(\text{NO}_3)_3$ oxidant (also can act as dopant) by rapid-mixing chemical oxidative polymerization with an external redox additive ($\text{CuSO}_4 \cdot 5\text{H}_2\text{O}$). A 0.1 M aniline solution was prepared and was stirred using magnetic stirrer for 15 min. To that, 1 M $\text{CuSO}_4 \cdot 5\text{H}_2\text{O}$ was added, and the aniline-copper mixture was stirred for half an hour. Finally, the oxidant 0.3 M ferric nitrate was rapidly added to the above aniline-copper solution. The reaction was kept overnight without any agitation. A dark green precipitate of polyaniline was filtered by using a vacuum pump and then washed with distilled water and acetone until the filtrate became colourless. Finally, it was dried in an air oven at 80°C for 24 h.

Material Characterization

The structural analysis was done by using Fourier transform infrared (FT-IR) spectroscopy (Thermo Nicolet, Avatar 370) and x-ray diffraction (XRD) analysis (Bruker AXS D8 Advance). Morphological characterisation was studied by using scanning electron microscopy (SEM) (TESCAN VEGA 3 SBH), SEM-EDS (OXFORD XMX N) and high-definition transmission electron microscopy (HD-TEM) (Jeol/JEM 2100). Dielectric and conductivity measurements were evaluated by using an Agilent LCR series meter-E4980 A from 100 Hz to 2 MHz on compressed PANI pellets at room temperature.

RESULTS AND DISCUSSION

Morphology (Scanning Electron Microscopy and Transmission Electron Microscopy)

The morphological analysis of the as-prepared PANI composites synthesized by using ferric nitrate oxidant with and without an external redox additive is depicted in Fig. 1. The above SEM images clearly show that with ferric nitrate oxidant PANI has highly irregular surface morphology. The addition of Cu^{2+} modified the morphology of PANI into a flake-like surface (supported by TEM analysis). The multiple coordination possibility of copper can provide inter- and intra-chain linkages among PANI chains to support the formation of flaky morphology thereby enhancing the conductivity and dielectric performance (supported by dielectric studies). Also, the flaky PANI composite can effectively carry the charges due to its high surface to volume ratio.

Further, the ability of ferric nitrate to act as both oxidant and dopant and the composition of the composite was studied by SEM-EDS analysis (SI-1). The polymerisation of aniline proceeds at a lower rate with $\text{Fe}(\text{NO}_3)_3$ since its redox potential (0.76 V) is lower than persulphate (2.0 V). When ferric nitrate was added to aniline solution, the oxidant itself gets reduced to ferrous nitrate ($\text{Fe}(\text{NO}_3)_2$) and the free ferric nitrate anions [$\text{Fe}(\text{NO}_3)_4^-$] formed act as a dopant for imine nitrogen in the PANI backbone (SI-2).⁹

Chemical Structure

Fourier Transform Infrared Spectroscopy (FT-IR)

The structural changes happened in PANI matrix synthesized with and without an external redox additive was investigated by using FT-IR spectroscopy and XRD analysis and is depicted in Fig. 2. The spectrum confirms the formation of conducting emeraldine salt form of the PANI composite. The FT-IR peaks around 1578 cm^{-1} , 1470 cm^{-1} , 1295 cm^{-1} and 1240 cm^{-1} represent characteristic peaks of conducting PANI and are assigned to C=C stretching vibration of quinoid diimine rings ($>\text{C}=\text{N}-$) and benzenoid diamine moieties, and those around and 1295 cm^{-1} and

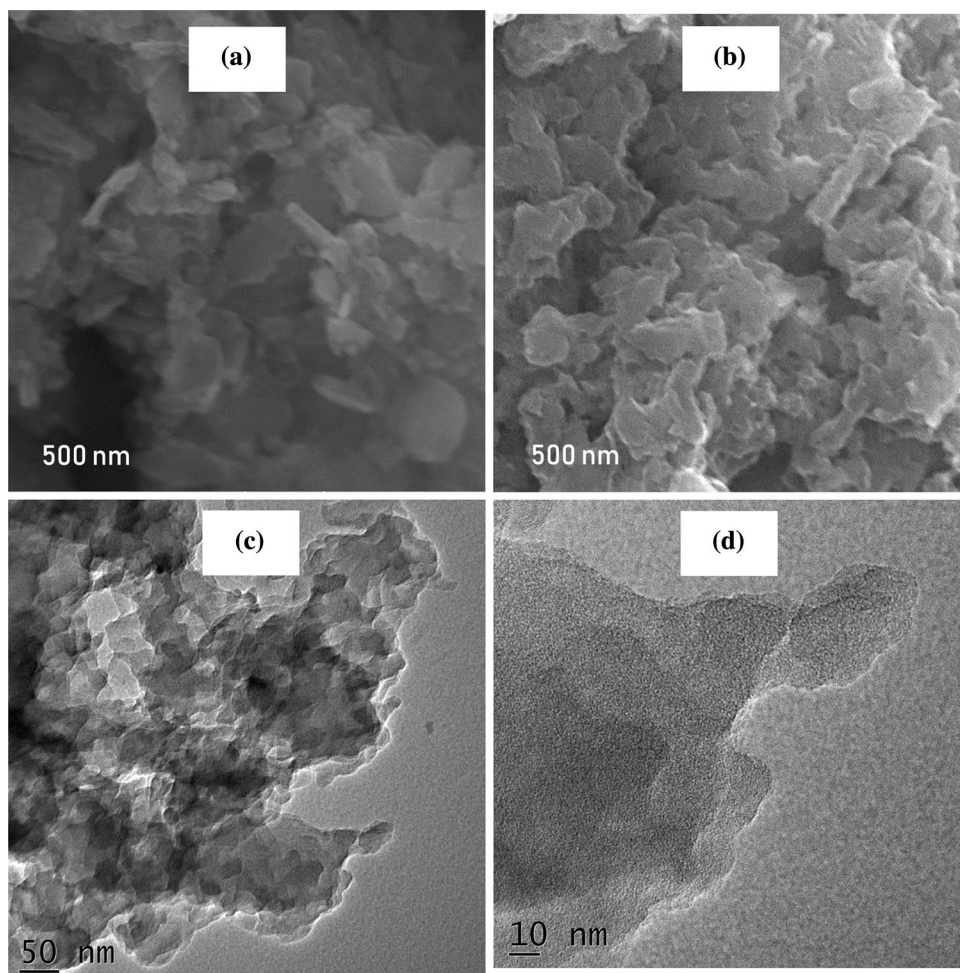


Fig. 1. SEM image of PANI composite (a) without an external redox additive, (b) with an external redox additive and TEM image with an external redox additive at (c) 50 nm, (d) 10 nm.

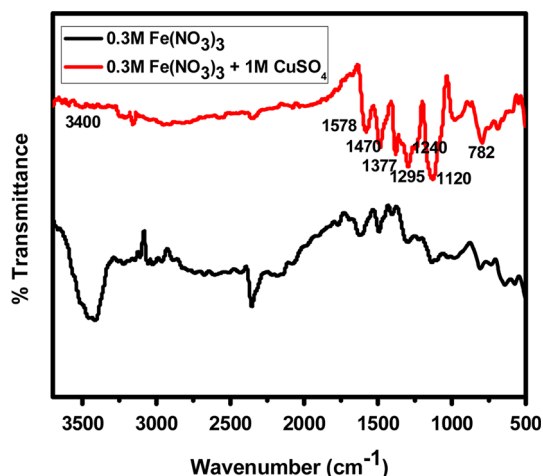


Fig. 2. FT-IR spectrum of PANI composite synthesized with and without an external redox additive.

1240 cm^{-1} represent C-N stretching vibrations of quinoid and benzenoid units. The sharp peak around 1120 cm^{-1} represents C-N stretching vibrations in B-NH⁺=Q (B-benzenoid, Q-quinoid). The

formation of 1,4 substituted phenylene rings is confirmed by the peaks centred around 782 cm^{-1} and out-of-plane C-H bending vibrations may result in many low-intensity peaks at lower wave numbers. Also, the presence of nitrate anion in the PANI matrix is confirmed by the N-O group absorption seen around 1377 cm^{-1} .¹⁰ The N-H stretching vibration of the PANI chain is indicated by the peak around 3400 cm^{-1} . The incorporation of Cu²⁺ in PANI matrix is clearly indicated by the diminished N-H stretching peak in the FT-IR spectrum of PANI with an external redox additive. Because of the formation of a coordinate bond between metals and nitrogen atoms, Cu²⁺ doped PANI shows broad peaks.

UV-Visible analysis

UV-Visible absorption spectroscopy analysis was done on the sample to analyze the electronic properties of the PANI composite and is shown in Fig. 3. The spectrum shows the three characteristics peaks of PANI at 360 nm, 424 nm and 658 nm. The pi-pi* transition of the benzene ring is indicated by the

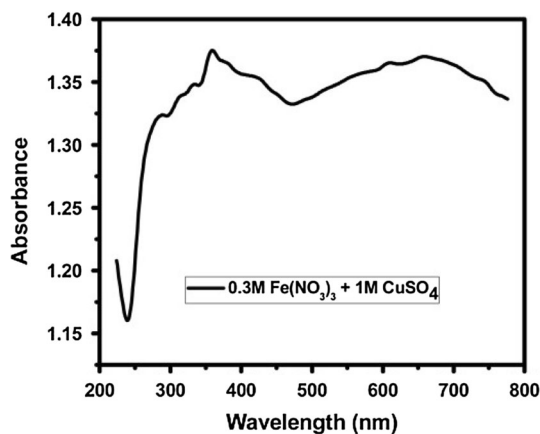


Fig. 3. UV–Visible spectrum of the PANI composite synthesized with an external redox additive.

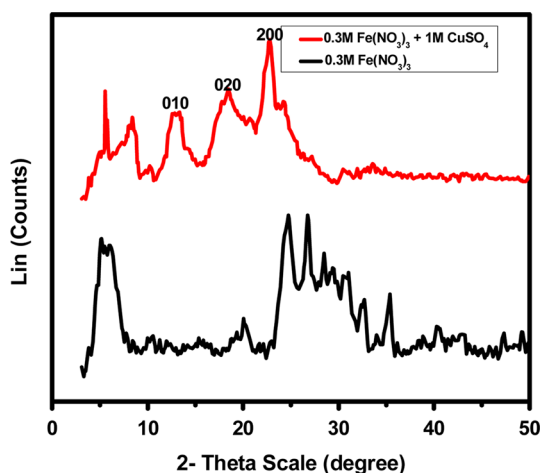


Fig. 4. XRD pattern of the PANI composite synthesized with and without an external redox additive.

peak around 360 nm, which is a HOMO–LUMO electronic transition. Also, the above peak is ascribed to the excitation of benzenoid units of PANI chains. The shoulder at 424 nm represents polaron- π^* transition of the protonated form of polyaniline. The long tail seen around 658 nm indicates n - π^* electronic transition of a benzenoid unit into quinoid moiety confirming the emeraldine salt structure of as-synthesized PANI.

X-ray Diffraction Analysis

Figure 4 represents the XRD pattern of PANI and Cu^{2+} added PANI synthesized using ferric nitrate oxidant. The characteristic peaks observed around 2theta values 20 and 25 in the XRD pattern are the characteristic peaks of the emeraldine salt form of PANI and is related to the periodicity parallel and perpendicular to the polymer chain, corresponding to (020) and (200) crystalline planes. The presence of peaks at lower 2theta values around 6 and 15 indicates highly ordered PANI chains and a (010) plane, respectively. Such lower diffraction peaks are

the result of the efficient penetration of dopants in the PANI matrix. The incorporation of the copper transition metal in the PANI matrix is confirmed by the broadened peaks observed in the XRD pattern of Cu^{2+} added PANI compared to that of the PANI composite without an external redox additive. The improved peak intensities observed in the case of Cu^{2+} added PANI may be related to the enhanced nucleation process in presence of copper.

Dielectric studies

Figure 5 shows the role of Cu^{2+} in enhancing the dielectric performance of the PANI composite in a frequency range 100 Hz–2 MHz. Dielectric constant and tangent loss values are calculated using the equations

$$\epsilon' = Cd/\epsilon^0 A \quad (1)$$

$$\tan\delta = \epsilon''/\epsilon' \quad (2)$$

where ϵ^0 is the dielectric permittivity in vacuum ($8.85 \times 10^{-12} \text{ Fm}^{-1}$), C capacitance, d thickness and A area of the pellet, ϵ' is the dielectric constant and ϵ'' is the dielectric loss. The degree to which the insulating material surface interacts with the electric field contributes towards dielectric constant and tangent loss is the amount of electrical energy escaped as heat.

For all the samples dielectric constant and tangent loss is high at lower frequency due to strong interfacial polarization¹ and then due to the accumulation of charge carriers at the internal interfaces called Maxwell–Wagner–Sillars effect a sharp decrease is observed. The relatively stable ϵ' and $\tan\delta$ values at high frequency portion arises from dielectric relaxation phenomenon. The doped PANI system comprises of mobile polaron-bipolaron system and the dipoles with restricted mobility. The improved ϵ' value of Cu^{2+} added PANI is attributed to the improved delocalization due to the interaction of binary metal cations with PANI chain and dipole and interfacial charge polarization between transition metals (Cu and Fe) and polymer¹⁰ which is an indication of better ability to store charges under the influence of an alternating field.¹¹ Also, the bipolaron structure formed from the close association of metal ions¹² could contribute towards the enhanced dielectric constant value of Cu^{2+} added PANI when compared to PANI synthesized without external an external redox additive. Also, the improved conductivity due to the addition of Cu^{2+} enhances the dielectric behaviour of the resultant PANI composite. The modified flaky morphology with its high surface-to-volume ratio due to the addition of Cu^{2+} further enhances the storage capacity. The high $\tan\delta$ value observed for Cu^{2+} -doped PANI is associated with free charge motion differences resulting in interfacial polymerization.¹³

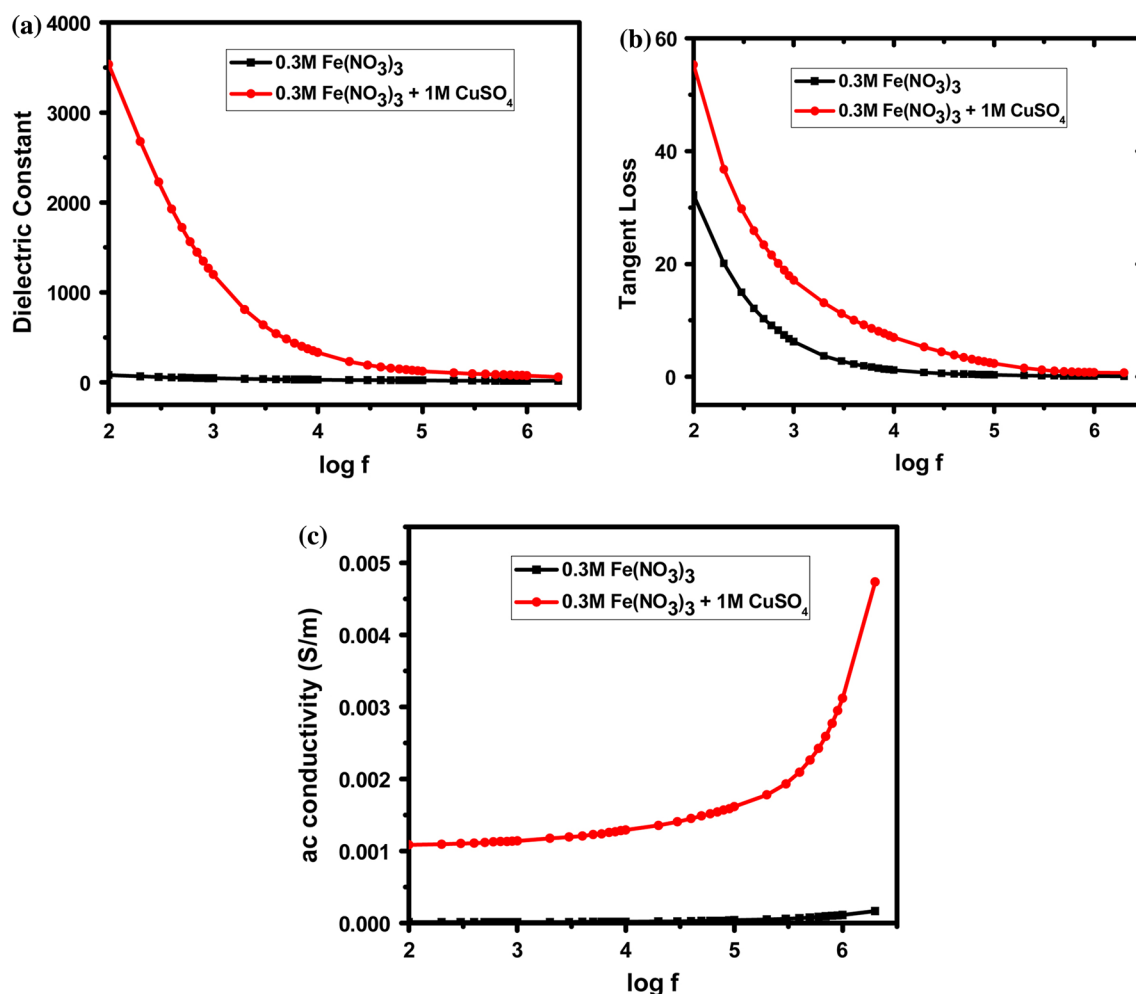


Fig. 5. Frequency dependence of (a) dielectric constant, (b) tangent loss, (c) ac conductivity.

AC conductivity is calculated using the equation

$$\sigma_{ac} = 2\pi f \epsilon'' \epsilon^0 \quad (3)$$

where $\sigma(ac)$ is the ac electrical conductivity (S/cm); f is the applied frequency (Hz); ϵ'' is the dielectric loss. Frequency dependent ionic conductivity and electronic hopping (electronic resonance) conductivity together contribute towards ac conductivity. The conductivity values increase with the increase in frequency. The long-range translational movement of charges is attributed to the frequency independent ac conductivity behaviour at the low frequency side.¹² From Fig. 3c it is clear that the conductivity of Cu²⁺ added PANI system is higher than those synthesized without an external additive due to the increased charge carriers, which provide a better conductive pathway.¹¹ Because of the accumulation

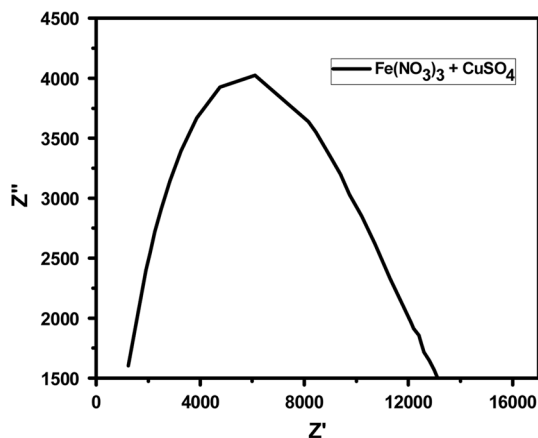


Fig. 6. Cole–Cole plot of PANI.

of mobile charges at the interfaces and dipole formation on metal complexes. Interface charge polarization (the Maxwell–Wagner–Sillars effect) and intrinsic electric dipole polarization is prominent on the metal-PANI system due to the coordination via nitrogen atoms, which finally contribute towards frequency dependent conductivity.^{11,12}

A Cole-Cole plot is a plot between complex permittivity (Z') on the X-axis and the imaginary part (Z'') on the Y-axis. This plot explains the polydispersive nature of dielectric relaxation. The above plot (Fig. 6) shows a circular arc indicating Debye-type relaxation of the PANI sample.

CONCLUSIONS

In summary, we have demonstrated an enhancement in the dielectric performance of binary transition metals embedded in a polyaniline composite synthesized using a ferric nitrate oxidant-dopant and Cu^{2+} as an external redox additive. The morphological study shows the importance of external Cu^{2+} additive on PANI surface to obtain a flake-like surface. Because of high surface-to-volume ratio, the flake-like PANI composite plays a significant role as an efficient charge carrier, thereby enhancing charge delocalization, conductivity and finally the dielectric performance. Thus, it is concluded that the as-synthesized PANI composite is an efficient dielectric material for energy storage applications.

ACKNOWLEDGMENTS

The authors acknowledge the director and principal, Rajagiri School of Engineering & Technology and Bharata Mata College for the support of this work. Analytical support from the Sophisticated Test and Instrumentation Centre, CUSAT, School of Pure & Applied Physics, Mahatma Gandhi University and Department of Physics, Maharajas College are also acknowledged.

CONFLICTS OF INTEREST

There are no conflicts to declare.

REFERENCES

1. W. Xu, Y. Ding, Y. Yu, S. Jiang, L. Chen, and H. Hou, *Mater. Lett.* 192, 25–28 (2017). <https://doi.org/10.1016/j.matlet.2017.01.064>.
2. X. Peng, Q. Wu, S. Jiang, M. Hanif, S. Chen, and H. Hou, *Mater. Lett.* 133, 240–242 (2014). <https://doi.org/10.1016/j.matlet.2014.07.017>.
3. E. Bhardwaj E, S. Prasher S, M. Kumar, U. Kaur U, M. Sahni, *J. Electron. Mater.* (2016). <https://doi.org/10.1007/s11664-016-5107-z>.
4. L. Ma, W.Y. Su, M.Y. Gan, X.F. Li, and L.Z. Luo, *J. Polym. Res.* 18, 595–599 (2011). <https://doi.org/10.1007/s10965-010-9453-x>.
5. S. Cho, M. Kim, J.S. Lee, J. Jang, and A.C.S. Appl, *Mater. Interfaces* 7, 22301–22314 (2015). <https://doi.org/10.1021/acami.5b05467>.
6. D. Ghosh, S. Giri, A. Mandal, and C.K. Das, *RSC Adv.* 3, 11676 (2013). <https://doi.org/10.1039/c3ra40955dl>.
7. L. Li, A.R.O. Raji, H. Fei, Y. Yang, E.L.G. Samuel, J.M. Tour, and A.C.S. Appl, *Mater. Interfaces* 5, 6622–6627 (2013). <https://doi.org/10.1021/am4013165>.
8. S. Dhibar, P. Bhattacharya, G. Hatui, S. Sahoo and C. K. Das, *Sustainable Chem. Eng.* (2014). <https://doi.org/10.1021/sc5000072>.
9. F. Zeng, Z. Qin, B. Liang, T. Li, N. Liu, and M. Zhu, *Prog. Nat. Sci. Mater. Int.* 25, 512–519 (2015). <https://doi.org/10.1016/j.pnsc.2015.10.002>.
10. Y. Zhang, C. Dou, L. Li, and Y. Wang, *Polym. Sci. Ser. A* 56, 146–151 (2014). <https://doi.org/10.1134/S0965545X14020138>.
11. J. Tahalyani, K.K. Rahangdale, R. Aepuru, B. Kandasubramanian, and S. Datar, *RSC Adv.* 6, 36588–36598 (2016). <https://doi.org/10.1039/C5RA23012H>.
12. M.D.A. Khan, A. Akhtar, and S.A. Nabi, *New J. Chem.* 39, 3728–3735 (2015). <https://doi.org/10.1039/C4NJ02260B>.
13. M. Niranjana, L. Yesappa, S.P. Ashokkumar, H. Vijeth, S. Raghu, and H. Devendrappa, *RSC Adv.* 6, 115074–115084 (2016). <https://doi.org/10.1039/C6RA24137A>.

Publisher's Note Springer Nature remains neutral with regard to jurisdictional claims in published maps and institutional affiliations.